Advanced Performance Materials, 2, 43–50 (1995)


# Effect of Ultrasonic Processing of Molten Metal on Structure Formation and Improvement of Properties of High-Strength Al-Zn-Mg-Cu-Zr Alloys

G.I. ESKIN, G.S. MAKAROV AND YU.P. PIMENOV
*All-Russia Institute of Light Alloys, Gorbunov St. 2, Moscow 121596, Russia*

**Abstract.** The ultrasonic treatment of molten and solidifying metal used along with other physical methods, such as thermal treatment, filtration, etc., enables one to obtain a nondendritic structure and uniformly disperse intermetallic particles in aluminum ingots. The structure and properties of ingots and extruded shapes from high-strength Al-Zn-Mg-Cu alloys (containing up to 0.3% Zr) are shown to be considerably improved after ultrasonic treatment.

**Keywords:** acoustic cavitation, intermetallic crystals, nondendritic structure, solidification nuclei

**Abbreviations:** F, fine filtration; HT, heat treatment; UST-1, ultrasonic treatment in a trough; T, undercooling of melt in a water-cooled tray; UST-2, combination of undercooling with ultrasonic treatment; UST-3, ultrasonic treatment in the liquid ingot bath; K, reference experimental results

## Introduction

The reliability and service life of components made of aluminum alloys are determined mainly by such properties as fracture toughness, fatigue endurance, fatigue crack growth rate, and corrosion resistance. An improvement of the mechanical properties of high-strength aluminum alloys occurs with the addition of zirconium. As an example, zirconium additions resulted in a nonrecrystallized structure in extruded items without a coarse-grained rim; the static strength, impact toughness, and fatigue endurance being increased [1–3].

Zirconium, being a powerful antirecrystallizing agent, to a great extent determines the microstructure of mill products having a significant influence on their corrosion resistance, in particular resistance against segregating and intergranular corrosion [3]. It is known that mill products of aluminum alloys containing 0.15% Zr possess increased resistance to segregating corrosion and higher resistance against corrosion cracking as compared with similar mill products made of an alloy containing only 0.1% Zr.

However, the positive effect of zirconium is significant only when it is present as uniformly distributed fine intermetallic particles in a homogeneous solid solution. It is known that zirconium has a relatively low solubility in solid aluminum [1]. On conventional casting, Zr addition of more than 0.15–0.20% results in the appearance of coarse primary intermetallics in the structure of ingots and mill products. Thus, the maximum improvement of aluminum alloy properties with a zirconium addition is achieved when a sufficiently high concentration of zirconium is present to give the desired fine intermetallic dispersion, while avoiding formation of coarse intermetallic inclusions in the as-cast structure. The present paper will address this situation.

V.I. Dobatkin [4] considered the process of primary intermetallic crystals formation and proposed two basic methods to suppress primary intermetallic solidification: (1) decrease the number of intermetallic solidification nuclei, and (2) the introduction of additional solidification sites to create a situation where a lack of material for intermetallic solidification prohibits the growth of intermetallic particles.

Among the various methods of grain refinement and suppression of primary $Al_3Zr$ solidification available in Al-Zn-Mg-Cu-Zr ingots, we have chosen the ultrasonic methods of molten alloy treatment under intensive acoustical cavitation [5–11]. Ultrasonic treatment of molten metal using multilayer screen filters (Usfirals-Process) results in a significant reduction in solid particles, and ultrasonic processing of molten metal in a liquid bath leads to grain refinement down to the level of nondendritic solidification.

In most cases of continuous casting, the primary solidification occurs on solid phase particles of a different type from that of the matrix melt, i.e., heterogeneously. It is well known that oxide particles and other microscopic nonmetallic compounds (so called "plankton") being wet by the molten metal and being crystallographically similar to the matrix operate as the solidification sites.

However, only a small proportion of the "plankton" are involved in the solidification, because nonmetallic particles as a whole are not wet by the molten metal due to surface defects (cracks, recesses, etc.) filled with gaseous phase, hence they do not participate in the solidification process. Previously [6–10], we have shown that a majority of the "plankton" particles are involved in the solidification if the molten metal is subjected to the acoustical cavitation during solidification.

The transition of inert particles into an active form is induced by acoustical cavitation with the following characteristics. When the ultrasonic intensity is higher that the cavitation threshold, a cavity containing a gaseous phase is formed close to the capillary surface, because precisely in this location the cavitation strength of the liquid metal is decreased due to the gaseous phase; i.e. the gaseous phase adjacent to the capillary surface of the non-metallic particles acts as the cavitation nucleation site. The cavity formed, as a rule, collapses after several cycles of nonlinear oscillations transform the stored energy either into high pressure pulses or powerful cumulative jets of liquid. This causes wetting of the impurities with molten metal despite the capillary limitations, and the molten metal solidifies after entering the capillary. This process can be considered as an activation of impurity particles, because the molten metal that solidifies in the capillary remains solid even at temperatures above the liquidus for a given alloy.

The solid phase formed in a capillary serves as a location for the formation of transition metal (TM) aluminides; the latter, in turn, acting as solidification sites.

Our studies have shown that the ultrasonic cavitation combined with the modification of the molten metal by the addition of a TM, e.g., $\geq$0.2% Zr, forms a sufficient amount of nuclei in the vicinity of the solidification front to result in the significant refinement of the grains and transition to nondendritic solidification which proceeds without primary solidification of coarse intermetallics.

Evidently, the nondendritic structure appears due to the presence of an extremely large numbers of potential solidification sites. In this case, the formation of solidification nuclei and the formation of dendritic arms occur at the same undercooling. As in the case of dendritic crystallization, the formation and growth of grains is controlled by the undercooling at the solidification front. The reduced undercooling adjacent to the growing nucleus prevents the formation and growth of new nuclei and formation of dendritic arms.

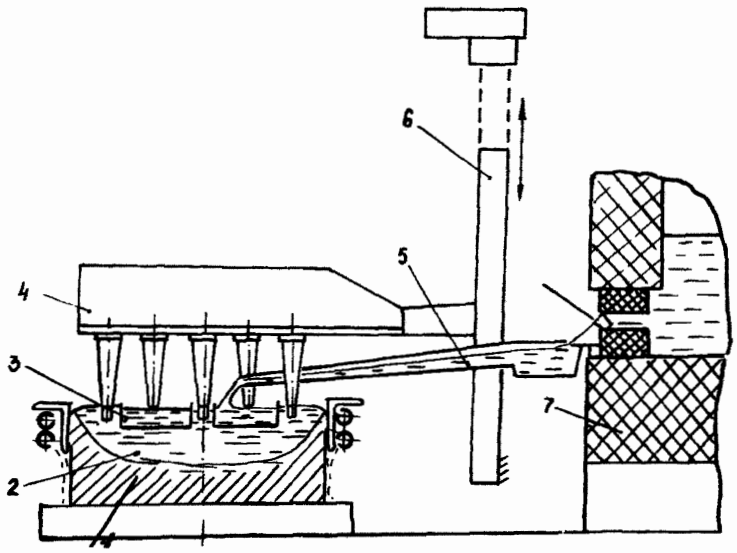


*Figure 1.* Schematic of large-scale ingot casting of aluminum alloys with ultrasonic processing of molten metal in the liquid bath: 1, ingot; 2, liquid bath; 3, distributing (casting) trough; 4, ultrasonic transducers; 5, casting tray; 6, moving mechanism for ultrasonic sources; and 7, holding furnace containing molten metal.

## Experimental results

The procedure of nondendritic solidification is widely used in continuous casting of light alloy ingots with small, medium, and large cross-sections [5–11]. In this case, the ultrasonic processing of molten metal is performed in the liquid bath of an ingot. Figure 1 shows a diagram of continuous casting with ultrasonic treatment of aluminum alloy ingots up to 1200 mm in diameter. The ultrasonic treatment under conditions of cavitation when applied to continuous casting of large-sized commercial ingots of Al-Zn-Mg-Cu or Al-Cu-Mg alloys with 0.13–0.14% Zr leads to the formation of the nondendritic structure, the nondendritic grain size being less than 150 $\mu$m. Transition to nondendritic solidification results in enhanced ductility in large-scale ingots, which is very important for casting and subsequent hot forming operations.

The ultrasonic treatment of solidifying large-sized ingots of aluminum structural alloys gives an increase of 1.5–2.0 times in the ductility at 20°C and in the temperature range of forming (Fig. 2).

Nondendritic solidification and the improvement of ductility of the as-cast metal has the major advantage of allowing an increase in the size of the cross-section of ingots produced from high-strength Al-Zn-Mg-Cu-Zr alloys without cracking [6–9, 11]. As an example, the maximum size of round ingots made of 1973 (7050) grade alloy containing Zr was successfully increased from 830 mm to 960 mm. This result cannot be obtained by other techniques.

The second important advantage of nondendritic crystallization is a "hereditary" formation of a refined grain structure and, hence, improved ductility of mill products produced by hot deformation, virtually independent of the deformation process used.

The mechanical properties obtained for a wide variety of mill products (stampings, forgings, massive shapes, slabs, etc.) from high-strength Al-Zn-Mg-Cu-Zr alloys show that

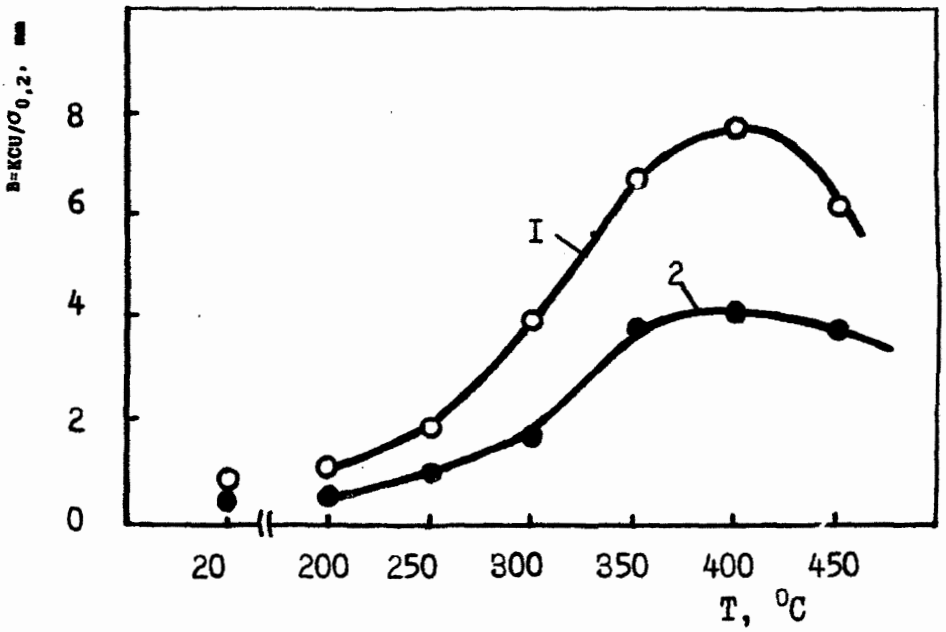


*Figure 2.* Effect of nondendritic structure on ductility in the hot-deformation temperature range (B = KCV/0.2% YS), where KCV is the impact toughness). Data for an ingot 830 mm in diameter from a 1973 grade alloy (Al-Zr-Mg-Cu-Zr) with 0.15% Zr: 1, casting with ultrasonic processing (nondendritic structure) and 2, casting without ultrasonic processing (dendritic structure).

*Table 1.* Effect of Ingot structure on height properties of small-size stamping and of large-sized extruded plates made of high-strength Al-Zn-Mg-Cu-Zr alloys.

| Ingot Structure | Stampings of 1960 grade alloy (Al-8.5%Zn-2.5%Mg-2.3%Cu-0.15%Zr) | | Extrusions of 1973 grade alloy (Al-6.0Zn-2.0%Mg-1.7%Cu-0.15%Zr) | |
|---|---|---|---|---|
| | UTS, MPa | El., % | UTS, MPa | El., % |
| Nondendritic | 600 | 5.1 | 484 | 3.8 |
| Dendritic | 540 | 3.2 | 474 | 2.4 |

Note: average data of 6 to 25 measurements

the nondendritic structure of an ingot decreases the microstructure and property anisotropy over a section of deformed metal, and further increases the ductility in a height direction without strength loss (Table 1). This latter fact is very significant.

The positive effect of a nondendritic structure on the quality of wrought Al-Zn-Mg-Cu-Zr alloys was confirmed by studying particular structure-sensitive properties such as stress-corrosion resistance, creep and fatigue endurance, fracture toughness, fracture crack propagation rate, etc. [6–11]. When the concentration of Zr in Al-Zn-Mg-Cu alloys exceeds

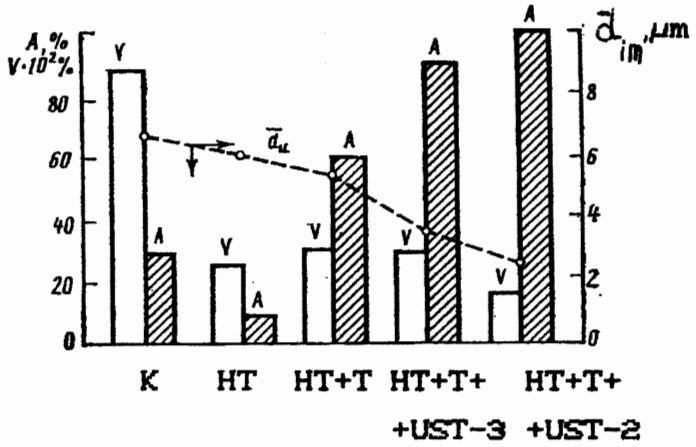


*Figure 3.* Effect of ultrasonic processing of molten metal in combination with other kinds of treatment on the structure of 1973 (0.3% Zr) ingots 145 mm in diameter (see explanations in text).

0.2%, the unavoidable primary solidification of $Al_3Zr$ lowers the metal quality. The size and volume fraction of primary intermetallics depends critically on the molten metal preparation and solidification conditions.

To suppress the primary solidification of intermetallics, we used (a) the filtration of molten metal through multilayer small-mesh screen filters (F), which resulted in the capture of solid nonmetallic particles up to 1 $\mu$m in size and (b) long-time heat-treatment of molten metal (HT) to deactivate impurities.

The number of solidification nuclei can be increased by the following methods: (a) the introduction of nucleation modifiers, (b) ultrasonic processing of molten metal in a trough (UST-1), (c) undercooling of a molten metal stream in a water-cooled tray (T), (d) a combination of undercooling and ultrasonic processing (UST-3), and (e) ultrasonic processing of molten metal in the liquid bath (UST-3). These methods were applied separately and in different combinations and compared with results obtained without additional processing (K).

We studied continuous casting into a sliding solidifier of ingots 145–270 mm in diameter. The ingot structure was studied to estimate the average size ($\bar{d}_{im}$), morphology and volume fraction ($v$) of $Al_3Zr$ primary intermetallics, proportion of nondendritic grains (A), and the Zr content in the matrix solid solution. The nondendritic grain fraction was evaluated in an optical microscope using the colored oxidation of specimens; the volume fraction of intermetallics was determined in a Quantimet-720 instrument; and the Zr concentration in solid solution was evaluated using a Supersonde GXA-733 setup.

The formation of coarse primary $Al_3Zr$ intermetallics in an ingot can be prevented by means of long-term heat treatment of the molten metal in a mixer. Long-time (up to 3.0 h) overheating of molten metal to 1000°C [12] should deactivate impurities and affect the primary $Al_3Zr$ intermetallic solidification. The results of long-term heat treatment in combination with cooling in the tray, ultrasonic processing in the trough, and ultrasonic processing in the bath during casting of 1973 alloy (0.3% Zr) ingots 145 mm in diameter are given in Fig. 3. The sequential influence of long-term heat treatment, stream undercooling, and ultrasonic processing of the molten metal decreases the intermetallic size and facilitates the nondendritic solidification.

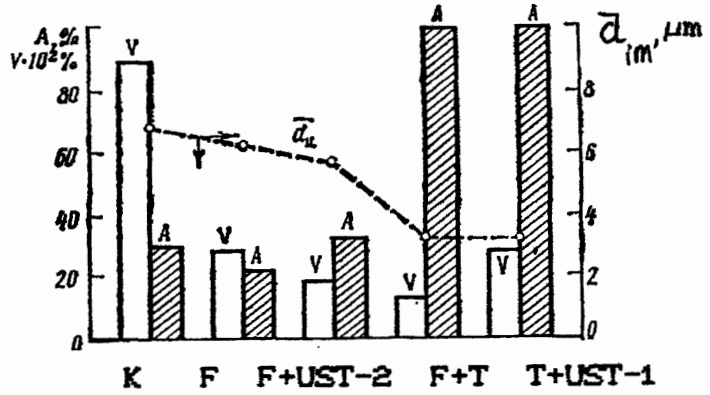


*Figure 4.* Effect of fine filtration (Usfirals-process) using multilayer screen filters (F) combined with other kinds of molten metal treatments on structure of 1973 (0.3% Zr) ingots, 270 mm in diameter (see explanations in text).

A more pronounced effect of molten metal preparation on the primary solidification can be observed in the structure of 270-mm diameter ingots processed using the fine filtration of molten metal in which the fine nonmetallic particles are effectively removed from the melt. These results are shown in Fig. 4.

Filtration through seven layers is so effective in purification of the melt that a nondendritic structure is difficult to obtain even using UST-2 and 0.25% Zr; the average intermetallic size is reduced and the volume fraction decreases from 0.855 to 0.199%. A five-layer filter used in combination with tray undercooling and UST-1 allows one to reduce the volume fraction and size of intermetallics as well as obtaining a completely nondendritic ingot structure.

Figure 5 shows that the average $Al_3Zr$ intermetallic size is decreased to 3.25–3.0 $\mu$m and, corresponding volume fraction to 0.13%, accompanied by the formation of a nondendritic structure with a grain size of $\leq$50 $\mu$m.

## Discussion

An analysis of the experimental results presented above allow us to postulate some general behavior characteristics.

Fine filtration of molten metal through multilayer screen filters is much more effective in removing solidification sites from the metal than the long-term overheating. The filtration through a seven-layer filter results in such an efficient purification of the melt that it is difficult to produce a nondendritic structure even when using the UST-2 mode. In contrast, the undercooling of a melt in the tray combined with the five-layer filtration assures a nondendritic structure.

The investigations have shown that the undercooling of molten metal in a tray (with and without UST-2) is an extremely effective method of nuclei formation (multiplication of solidification sites) and thus is a very efficient method for producing nondendritic solidification, refinement of intermetallics, and reduction of their volume fraction. The average $Al_3Zr$ size is reduced to 3–4 $\mu$m with a volume fraction of only 0.15–0.28% as compared with the reference experiment in which the average size is 6 $\mu$m and the volume fraction of

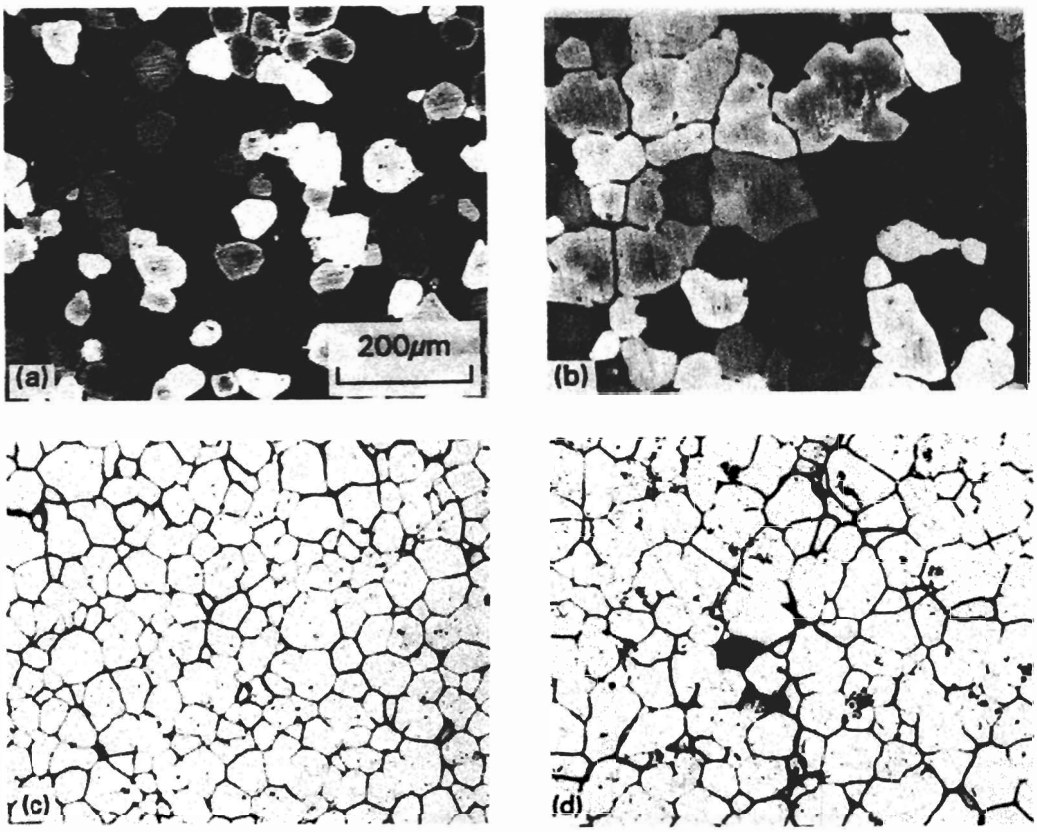


*Figure 5.* Grain structure of 1973 (0.3% Zr) ingots 270 mm in diameter (a, b ×100) and intermetallic particles (c, d ×100) in a standard process (b, d) and after the following treatment of the molten alloy: F + T + UST-2 (a, c).

primary intermetallics can reach 0.9%. Moreover, it must be noted that ultrasonic processing of molten metal also retards the growth of primary intermetallic crystals in the liquid bath due to additional overheating of the melt (by 20–25°C). This promotes the nondendritic solidification of ingots [5–6].

It can be assumed that such methods of casting and solidification (filtration, tray undercooling, ultrasonic processing) ensure a considerable reduction of the intermetallic $Al_3Zr$ volume fraction and, hence, should increase the Zr concentration in the solid solution. This is confirmed by electron-probe investigations which have shown that a reduced volume fraction ($v$) and average size ($\bar{d}_{im}$) of the intermetallics typical of nondendritic solidification, accompany an increase in the Zr content in the solid solution (Table 2).

Figure 5c, d shows the distribution of primary intermetallic sizes in 1973 alloy ingots of 270 mm diameter. The ingots have both dendritic and nondendritic structures. The fine filtration, undercooling in the trough, and ultrasonic treatment when applied in combination can decrease the maximum intermetallic size to 10 $\mu$m, up to 80% of the $Al_3Zr$ particles being less than 5 $\mu$m in size. In this case, $Al_3Zr$ primary particles are of the same size as basic alloy element particles. A reference ingot produced without use of the methods

*Table 2.* Degree of nondendritic solidification (A) as effected by average size of $Al_3Zr$ crystals ($\bar{d}_{im}$), volume fraction ($v$) and concentration of Zr in solid solution.

| A, % | $d_{im}$, $\mu$m | v, % | Concentration of Zr in Solid Solution, % |
|---|---|---|---|
| 30 | 6.80 | 0.855 | 0.067 |
| 80 | 3.65 | 0.290 | 0.073 |
| 100 | 3.25 | 0.129 | 0.110 |

discussed in the present work contains intermetallics with maximum size ($d_{im}$) of 20–25 $\mu$m and the average size ($\bar{d}_{im}$) is 6.8 $\mu$m.

These results are obtained for small-scale (270 mm) ingots, from alloys containing up to 0.3% Zr. It can be expected that ingots to 300–400 mm in diameter will behave in a similar manner at lower Zr content, in the range 0.15–0.17%.

The "hereditary" influence of increased Zr concentration (up to 0.3%) has been evaluated for extruded strips 40 × 200 mm in cross-section produced from 1973 ingots containing dispersed $Al_3Zr$ intermetallics, and compared with a similar strip obtained using the conventional 1973 alloy with 0.12% Zr. While tensile properties of extruded mill products in the longitudinal and transversal directions differ only by 10–15%, the low-cycle fatigue endurance ($\sigma_{max}$ = 160 MPa) is increased from 110 to 200 kilocycles with a simultaneously improved stress-corrosion resistance (the stress corrosion resistance parameter increases from 150 to 200 MPa).

## References


1. Elagin, V.I. 1975. Alloying of Wrought Aluminum Alloys with Transition Metals. Moscow: Metallurgiya.
2. Drits, A.M., Shneider, G.L., Vovnyanko, A.G., and Rudoi, A.V. 1988. Structure and Mechanical Properties of Extruded and Rolled Semifinished Items [Mill Products] of Al-Zn-Mg-Cu-Zr Alloys. *Izv. Akad. Nauk SSSR, Met.*, 6:149–152.
3. Valkov, V.D. 1982. Effect of Zirconium on Corrosion Resistance of Extruded Semifinished items [Mill Products] of D16ch alloy, *Tekhnol. Legk. Spl.*, 1:55–59.
4. Dobatkin, V.I. 1961. Aluminum Alloy Ingots. Moscow: Metallurgizdat.
5. Dobatkin, V.I. and Eskin, G.I. 1985. Physical Metallurgy of Aluminum Alloys. (S.T. Kishkin, (ed.)) Moscow, Nauka, 161–172.
6. Eskin, G.I. 1988. Ultrasonic Treatment of Molten Aluminum. Moscow: Metallurgiya.
7. Eskin, G.I., Pimenov, Yu.P., and Makarov, G.S. 1989. Effect of Combined Treatment of Molten Metal Upon Primary Crystallization [Solidification] in 1973 Grade Aluminum Alloy Ingots. *Izv. Akad. Nauk SSSR, Met.*, 4:87–91.
8. Eskin, G.I. 1993. Proc. Intern. Symp. on Light Mater. for Transp. Syst. (N.I. Kim, (ed.)) Kyongju, Korea: PUST, 585–593.
9. Belov, A.F., Dobatkin, V.I., and Eskin, G.I. 1992. Physical Metallurgy and Processing of Nonferrous Alloys. (A.F. Belov, (ed.)) Moscow: Nauka, 66–76.
10. Eskin, G.I. and Borovikova, S.I. 1993. Effect of Billet Structure on Quality of Stamped Semifinished Items [Mill Products] of High-Strength Al-Zn-Mg-Cu-Zr Alloys. *Metalloved. Term. Obrab. Met.*, 6:18–20.
11. Eskin, G.I. 1994. Influence of Cavitation treatment of Melts on the Processes Nucleation and Growth of Crystals During Solidification of Ingots and Castings from Light Alloys. *Ultrasonics Sonochemistry*, 1:59–63.
12. Kisun'ko, V.Z. 1980. Thermal-Rate Refinement of Aluminum Alloys. *Izv. Akad. Nauk. SSSR, Met.*, 1:125–127.

Available online at www.sciencedirect.com
SCIENCE DIRECT
ELSEVIER
Materials Letters 59 (2005) 190–193
materials letters
www.elsevier.com/locate/matlet

# Effect of power ultrasound on solidification of aluminum A356 alloy

X. Jian[a], H. Xu[a], T.T. Meek[a], Q. Han[b,*]

[a]*Material Sci. and Eng. Department, University of Tennessee, Knoxville, TN 37996, USA*
[b]*Oak Ridge National Laboratory, Oak Ridge, TN 37831-6083, USA*

Received 29 March 2004; received in revised form 18 June 2004; accepted 25 September 2004
Available online 12 October 2004

**Abstract**

The present investigation attempted to evaluate the effect of ultrasonic vibration on the nucleation and growth of aluminum alloy A356 melt. A356 melt was treated at various solid fractions isothermally with ultrasonic vibrations by dipping the acoustic radiator into the melt. Experimental result confirmed that globular grains could be effectively obtained when the melt was ultrasonically treated at the temperature close to its liquidus and subsequently cooled quickly. It further illustrated the difficulty to form globular grains when the specimens were treated at isothermal temperatures in the mushy zone. It may imply that in the given experiments cavitations-induced heterogeneous nucleation plays a more important role than dendrite fragmentation in the formation of globular grains.


*Keywords:* Solidification; Aluminum alloy; Ultrasonic vibration; Nucleation; Dendrite fragmentation

## 1. Introduction

The research of ultrasonic vibration for metallurgical applications can be dated back to 1878 when Chernov proposed the original idea of improving cast metal quality by elastic oscillations [1]. The injection of ultrasonic energy into molten alloys brings about nonlinear effects such as cavitation, acoustic streaming, emulsification, and radiation pressure [2], which are used to refine microstructures, reduce segregation, and improve secondary phase formation and distribution.

Ultrasonic treatment of aluminum alloys, in general, has been studied extensively [1,3–6]. It has been shown that the introduction of high intensity ultrasonic vibration into the melt can eliminate columnar dendritic structure, refine the equiaxed grains, and under some conditions, produce globular non-dendritic grains [1]. Mechanisms for grain refinement under ultrasonic vibrations have been proposed [7,8]. They are related to ultrasonically induced cavitations, which produce large instantaneous pressure and temperature fluctuations in the melt. These pressure and temperature fluctuations are likely to induce heterogeneous nucleation in the melt. They are also likely to promote dendrite fragmentation by enhancing solute diffusion through acoustic streaming. However, there is no convincing evidence in the literature as to which mechanism, i.e. heterogeneous nucleation or dendrite fragmentation, is more important for grain refinement under ultrasonic vibrations. This article reports some results of the carefully designed experiments in which ultrasonic energy was injected in the melt at various stages of solidification.

## 2. Experiments

The raw material used in this study was aluminum alloy A356 (Al–7.0 wt.% Si–0.4 wt.% Mg–0.1 wt.% Fe). The ultrasonic system used for this research consisted of a 1.5 kW acoustic generator, an air-cooled 20 kHz transducer made of piezoelectric lead zirconate titanate crystals (PZT), and an acoustic radiator made of titanium alloy Ti–6Al–4V. A pneumatically operated device was installed to move the radiator. The time to preheat the radiator and to dip it into the melt can be precisely controlled.

* Corresponding author. Tel.: +1 865 574 4352; fax: +1 865 574 4357.
*E-mail address:* hanq@ornl.gov (Q. Han).

0167-577X/$ - see front matter © 2004 Elsevier B.V. All rights reserved.
doi:10.1016/j.matlet.2004.09.027

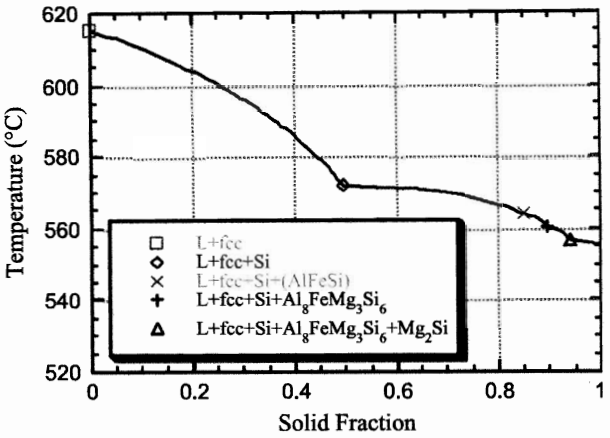


Fig. 1. Temperature versus solid fraction curve of A356 aluminum alloy.

The temperature versus solid fraction curve of this material was determined by thermodynamic simulations ahead of the experiments. As is shown in Fig. 1, the liquidus temperature of this alloy is 614 °C and the solidus temperature is 554 °C. The primary fcc aluminum dendrites start to form at 614 °C and the binary eutectics at 574 °C. Tertiary eutectics and complex intermetallics form at the late stage of solidification.

Three types of experiments were carried out, namely continuous processing, intermittent processing, and isothermal processing. In the continuous processing, ultrasonic energy was injected into the molten aluminum over a range of temperature that covered from 634 to 574 °C as the alloy cooled in the furnace. The ultrasonic system was not able to function when the melt temperature was lower than 574 °C since the solid fraction was too high. The second approach, intermittent processing, was the stepwise application of acoustic power coupled into the melt at different temperature intervals from 614 to 574 °C. Temperature intervals were 5 °C and the time of each isothermal treatment was varied over, 5, 10, and 20 s. The third approach consisted of isothermally applying acoustic energy into the melt at different solid fractions. The isothermal processing time varied from 5, 10, and 20 s. Experimental results reported in Ref. [9] indicate that 20 s is enough to produce globular grains during solidification of aluminum alloys.

In the experiments, aluminum A356 alloys were heated up to 650 °C and cooled to predetermined temperatures for ultrasonic processing. Meanwhile the ultrasonic radiator was also preheated to the same temperature as the aluminum melt. The radiator was then inserted into the melt. The specimens thus treated were cooled in the furnace to room temperature. The microstructure of the specimens was characterized.

## 3. Results and discussion

Fig. 2 shows the comparison of the obtained microstructure without (a) and with (b) the continuous application of acoustic power. Without acoustic vibration, the microstructure was dendritic and its average grain size was several millimeters. Upon the application of acoustic power, the dendritic structure was broken up into a somewhat globular grain structure. The average grain size was about 200 μm. This result is in accordance with previous work [7].

Microstructures corresponding to different intermittent time processing are presented in Fig. 3. The comparison between Figs. 2a and 3 reveals a very large difference in the resultant microstructure. In particular, the application of intermittent acoustic energy makes the microstructure more globular and destroys the dendritic microstructure. The comparison of Figs. 2b and 3 shows little difference in terms of grain morphology between the application of intermittent and continuous acoustic power. However, the average grain size appears to be reduced by intermittent acoustic vibration. Fig. 3 indicates that the intermittent treatment is more efficient than the continuous treatment in terms of grain size reduction. This is due to the fact that the cooling rate in the specimen treated with intermittent vibration is faster than that treated with continuous vibration. Cooling rate has a major effect on the resultant grain size.

Isothermal processing was then carried out in the melt. Fig. 4 shows the microstructure obtained for five conditions: without acoustic power applied (a); acoustic power applied 10 s at 614 °C (b), at 610 °C (c), at 605 °C (d). Isothermal processing reduces the average grain size compared with that without acoustic vibrations. The

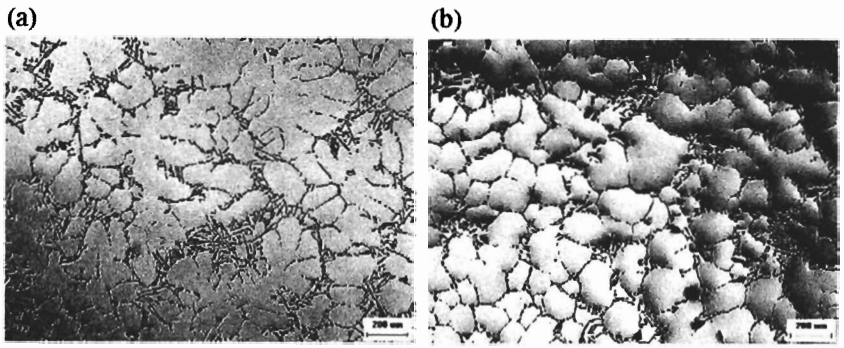


Fig. 2. A comparison of microstructures obtained without (a) and with (b) the application of continuous acoustic power.

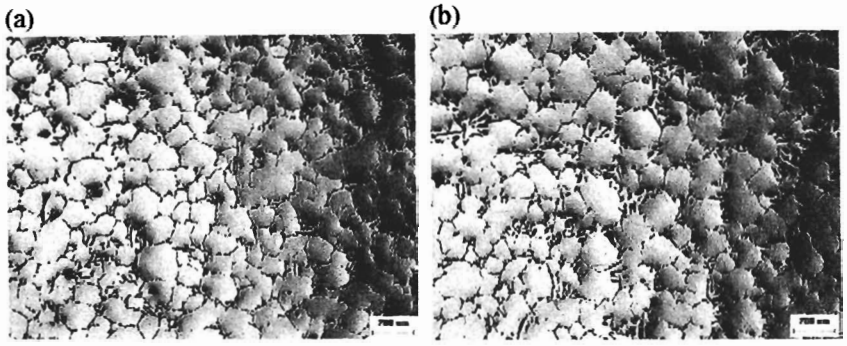


Fig. 3. A comparison of microstructures obtained with the application of intermittent acoustic power for (a) 10 s and (b) 20 s at each isothermal temperature step.

comparison of Fig. 4b with c shows little effect of processing temperature on the average grain size using isothermal processing. No globular structures were obtained for isothermal processing for various times and temperatures in the range of 614 to 574 °C.

Note that 614 °C is the liquidus temperature of the alloy; 610 and 605 °C are the temperatures where the corresponding solid fraction is about 0.1 and 0.18, respectively.

Finally, the isothermal processing time was increased. Fig. 5 shows the resultant microstructure of a specimen subjected to ultrasonic vibrations for 20 s at 614 °C (a) and 610 °C (b). The extended isothermal vibration time seems to have little effect on breaking up dendritic structures further and forming globular structures.

It is well known that isothermal coarsening can be used to produce a globular microstructure in aluminum alloy if the specimen is held at a semi-solid temperature for an extended time. Electromagnetic stirring can also be applied to a solidifying alloy to obtain globular grains at fairly short processing times. In fact, both isothermal coarsening and electromagnetic stirring have been successfully used for the production of globular/non-dendritic microstructures. The results shown in Figs. 4 and 5 suggest that it is difficult to obtain globular grains, in a short time frame, by injecting acoustic energy into aluminum A356 alloy in the semi-solid temperatures (mushy zone temperatures). This may imply that the temperature/pressure fluctuations induced by acoustic vibration are not efficient in breaking up dendrites in the mushy zone. Dendrite fragmentation requires the remelting of the secondary dendrite at their roots. Remelting of a solid is usually slow because latent heat is needed to remelt the secondary dendrites at their roots. The temperature/pressure fluctuations occur at a frequency of 20 kHz, which may be too fast for dendrite fragmentation. Some limited dendrite fragmentation occurred in our experiments since the grain size is reduced with acoustic vibration. The

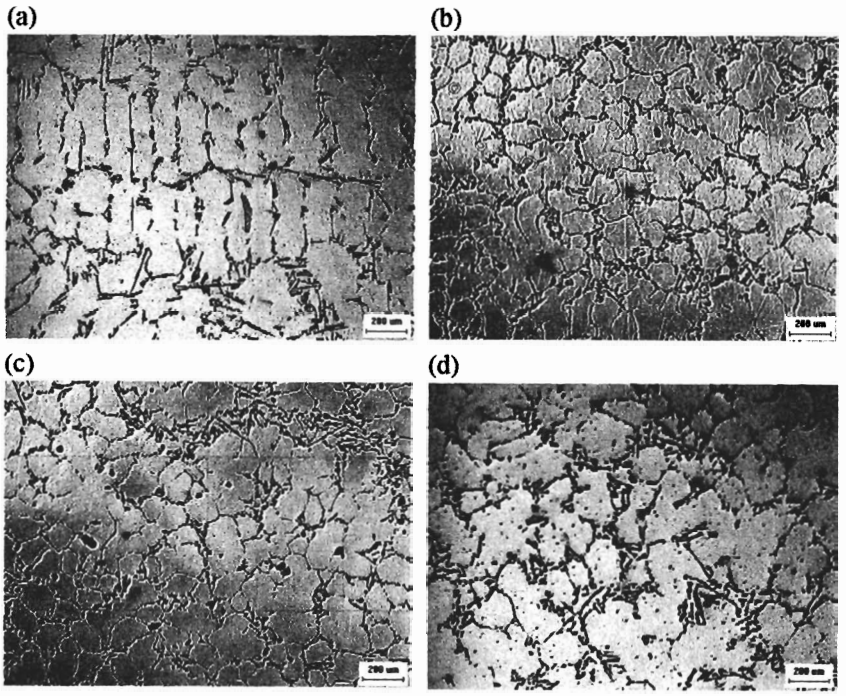


Fig. 4. A comparison of microstructures obtained without (a) and with isothermal processing for 5 s at 614 °C (b), at 610 °C (c) and at 605 °C (d).

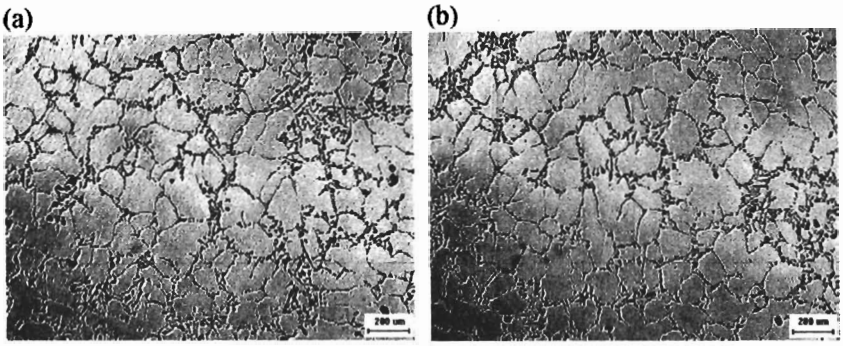


Fig. 5. The microstructures of specimens subject to ultrasonic vibration for 20 s under isothermal processing conditions at (a) 614 °C and (b) 610 °C.

limited dendrite fragmentation can be related to the acoustic streaming in the slurry, which promotes mass transfer and thus the remelting of dendrites at their roots.

Having excluded the effect of dendrite fragmentation on the formation of globular/non-dendrite microstructure in the acoustically processed melt, in this situation acoustically induced heterogeneous nucleation seems to be the dominant mechanism for the formation of a globular microstructure. With ultrasonic vibration applied to the melt, cavitations form, which give rise to the formation of a large number of tiny discontinuities or cavities. These cavities expand and collapse instantaneously. During the expansion stage of the small cavities, the temperature of the cavity surface drops. As a result, undercooling occurs on the cavity surfaces and results in the formation of nuclei of the solid phase. The formed nuclei can be distributed throughout the melt by the acoustically induced streaming. A large number of nuclei can be produced during the expansion stage, resulting in the formation of globular grains.

## 4. Summary

A globular/non-dendritic microstructure was obtained and grains were refined in the melt subjected to a continuous acoustic vibration when the melt was cooled from 634 to 574 °C. Better results were obtained by intermittent injection of acoustic energy in the melt. Isothermally ultrasonic treatment with a short time in the mushy zone reduced the average grain size but failed to produce a globular microstructure. This may suggest that in the given experiments the dominant mechanism for grain refinement using acoustic vibrations is likely not due to dendrite fragmentation but cavitation-induced heterogeneous nucleation.

## Acknowledgments

This research was supported by the United States Department of Energy under Contract No. DE-PS07-02ID14270 with UT-Battelle, LLC.

## References

[1] G.I. Eskin, Ultrasonic Treatment of Light Alloy Melts, Gordon & Breach, Amsterdam, 1998, p. 1.
[2] O.V. Abramov, Ultrasonics 25 (1987) 73.
[3] G. Brodova, P.S. Popel, G.I. Eskin, Liquid Metal Processing, Taylor & Francis, New York, 2002.
[4] J. Campbell, International Metals Reviews 2 (1981) 71.
[5] V.O. Abramov, O.V. Abramov, F. Sommer, D. Orlov, Materials Letters 23 (1–3) (1995) 17.
[6] G.I. Eskin, Ultrasonics Sonochemistry 8 (3) (2001) 319.
[7] G.I. Eskin, Ultrasonics Sonochemistry 1 (1) (1994) S59.
[8] V. Abramov, O. Abramov, V. Bulgakov, F. Sommer, Materials Letters 37 (1–2) (1998) 27.
[9] C. Liu, Y. Pan, S. Aoyama, in: K. Bhasin, et al., (Eds.), Proceedings of the 5th International Conference on Semi-Solid Processing of Alloys and Composites, Colorado School of Mines, Golden, CO, 1998, pp. 439.

# Cavitation mechanism of ultrasonic melt degassing

**G.I. Eskin**

All-Russia Institute of Light Alloys, Gorbunov St. 2, Moscow 121596, Russia

*Received 1 October 1994*

The real melt always contains non-wettable fine inclusions which are potential nuclei for cavitation and degassing. This paper deals with the nature of ultrasonic degassing and the industrial application of a relevant technology.

**Keywords: acoustic cavitation; cavitation and degassing nuclei; ultrasonic degassing**

The degassing of liquids and low-melting melts under action of ultrasound was among first effects revealed in the 1930s[1-4]. We started own investigations on the mechanism of ultrasonic degassing of light alloy melts and began the industrial application of ultrasonic-induced degassing in the 1960s[3,5]. These investigations showed that hydrogen could be efficiently removed from Al- and Mg-based melts only when the ultrasonic treatment is accompanied by developing cavitation. It was shown that the ultrasonic degassing of liquid metals differed essentially from that of aqueous solutions and organic liquids. This is due to the different nature of cavitation nuclei and, hence, different conditions required for the origination and development of acoustic cavitation.

In the case of water and organic liquids, the cavitation nuclei are represented by solid inclusions and very fine gaseous bubbles. In contrast, only fine solid particles (mainly oxides, e.g. $Al_2O_3$ in aluminium melts) can act as cavitation nuclei in metallic melts.

## Cavitation and degassing nuclei

Owing to its nature, any metallic melt always contains a suspension of submicroscopic particles that are non-wettable by the melt and containing a gaseous phase in surface defects. This 'plankton' produces potential cavitation nuclei. The proportion of free hydrogen on the surface of these particles is very small, less than 0.1%. Nevertheless, this amount is sufficient to initiate cavitation. The transformation of cavitation bubbles into gaseous bubbles depends on the dynamics of cavitation bubbles and the diffusion-induced penetration of dissolved hydrogen into pulsing cavitation bubbles. Hydrogen bubbles thus formed can coarsen and, on reaching a certain size, float up to the surface of a liquid bath.

Earlier, we have shown[5,6,8-10] that real melts always contain oxide particles that are non-wettable by the melt and adsorbed hydrogen in surface defects of these particles. Under ultrasonic treatment, the amount of these particles and the content of adsorbed hydrogen become sufficient for simultaneous cavitation and ultrasonic-induced degassing.

## Diffusion growth of cavitation bubbles

The diffusion growth of bubbles in an ultrasonic field is one of the most interesting features of acoustic cavitation in metallic melts. In the absence of the acoustic field, the gaseous bubble should slowly dissolve owing to the gas diffusion from the bubble to the melt[5,6]. The situation changes dramatically when the surface of the bubble pulsates.

Under cavitation ultrasonic treatment, the diffusion of gas occurs in a unique direction, from the liquid to the bubble. This directed diffusion, being superimposed with the usual static gas diffusion from the bubble to the liquid, can greatly improve the gas motion to the bubble, especially when the sound pressure is over the cavitation threshold.

Directed diffusion can be considered on the basis of the following three effects of cavity pulsation:

1 The gas diffusion from the bubble to the liquid is directed when the cavity is compressed and the content of gas inside is increased.
2 During cavitation pulsation, the surface of the expanded bubble is much higher than that of the compressed bubble. Hence the amount of gas that enters the bubble during its extension is higher than the amount of gas leaving the bubble upon its compression.
3 The diffusion is controlled by the thickness of a diffusion layer that is formed in liquid enveloping the bubble. When the bubble is compressed, this layer grows and the concentration gradient decreases. Upon extension, the layer becomes thinner and the


*SSDI* 1350-4177(95)00020-8

concentration gradient increases. In this case, the flow-rate of gas to the bubble also increases.

The behaviour of bubbles during cavitation should be considered in terms of the changing amount of gas inside bubbles on their extension and collapse. In the general case, this process can be described using a complex system of equations.

We tried to simplify the problem[5,6]. Assuming that the bubble pulsates in non-condensable liquid, the time dependence of the bubble radius $R(t)$ can be expressed in terms of the Rayleigh (Noltingk–Neppiras) equation. Hence, the variation in amount of gas inside the bubble or the internal gas pressure $P(t)$ can be given by a non-linear dependence on the radius.

Assuming that the amount of gas inside the bubble is $M = 4\pi R^3 m\gamma/3$ (where $\gamma$ is the gas density inside the bubble and $m$ is the molecular weight of the gas), the variation in the amount of gas is

$$(4/3\pi)\mathrm{d}(\gamma R^3)/\mathrm{d}t = 4\pi R^2 i(t) \quad (1)$$

where $i(t)$ is the density of gas flow through the bubble surface. If the gas inside the bubble is ideal, then $P = \gamma kT$ (where $T$ is the absolute temperature of the gas in the bubble, which depends on time, and $k$ is the Boltzmann constant).

Assuming that the cavitation occurs under isothermal conditions, Equation (1) becomes

$$(R/3kT)\partial P/\partial t + P\partial R/(\partial tkT) = i(t) \quad (2)$$

The gas flow into the bubble can occur by several mechanisms, but diffusion is the major one. The following expression was proposed by Boguslavskii[7] to describe the density of gas flow into the bubble:

$$i = (8/3)\sqrt{5\pi}Z/\rho D^{1/2}C_0 t^{3/2} \quad (3)$$

where $Z = 0.8P_s$ ($P_s$ is the amplitude of sound pressure), $\rho$ is the density of liquid aluminium, $D$ is the diffusion coefficient of hydrogen in liquid aluminium, $C_0$ is the content of hydrogen in liquid aluminium and $t$ is the period of bubble pulsation.

Let the surface area of the bubble $S = 4\pi R^2$ be the unknown in the equations of bubble pulsation and gas diffusion into the pulsating bubble. In this case, the system of equations that describes the bubble dynamics and gas diffusion into the pulsating bubble is as follows:

$$\begin{cases} \partial^2 S/\partial t^2 = -(1/4)S(\partial S/\partial t)^2 + 2\pi/\rho[P(t) - P_0 - P_s \sin \omega t] \\ \qquad -4\sigma\pi^{3/2}/S^{1/2} - 4\mu\dot{S}/S \\ 3S^{3/2}/\sqrt{\pi}kT(\partial P/\partial t) + PS^{1/2}/2\sqrt{\pi}kT(\partial S/\partial t) = i \end{cases} \quad (4)$$

where $\rho$, $\sigma$ and $\mu$ are the density, surface tension and viscosity of the aluminium melt.

This system of equations was solved using numerical methods and computer software. $S(0) = S_0$, $P(0) = P_0$ and $\dot{S}(0) = 0$ were used as the initial conditions at $C_0 = 0.2$ cm$^3$ per 100 g and $D = 1$ cm$^2$ s$^{-1}$ for various starting radii of the cavitation bubble $R_0$. Bubbles 1–10 $\mu$m in radius were examined. These values reflect real dimensions of cavitation nuclei (non-wettable particles of alumina).

*Figure 1* shows the variations in the relative radius $R/R_0$ and in the hydrogen pressure inside the pulsating bubble $P_g$ (bubble radius $R_0 = 10$ $\mu$m) at three applied pressures $P_s$: 0.2 MPa (no cavitation occurs), 1.0 MPa (the cavitation threshold) and 10 MPa (developed cavitation). Note that the flow of hydrogen into the bubble increases with cavitation development and sound pressure build-up. The bubble pulsation before cavitation changes the gas pressure only slightly (*Figure 1a*). At the cavitation threshold (*Figure 1b*), the hydrogen pressure inside the bubble changes by three orders of magnitude. Finally, the diffusion of hydrogen under cavitation pulsation

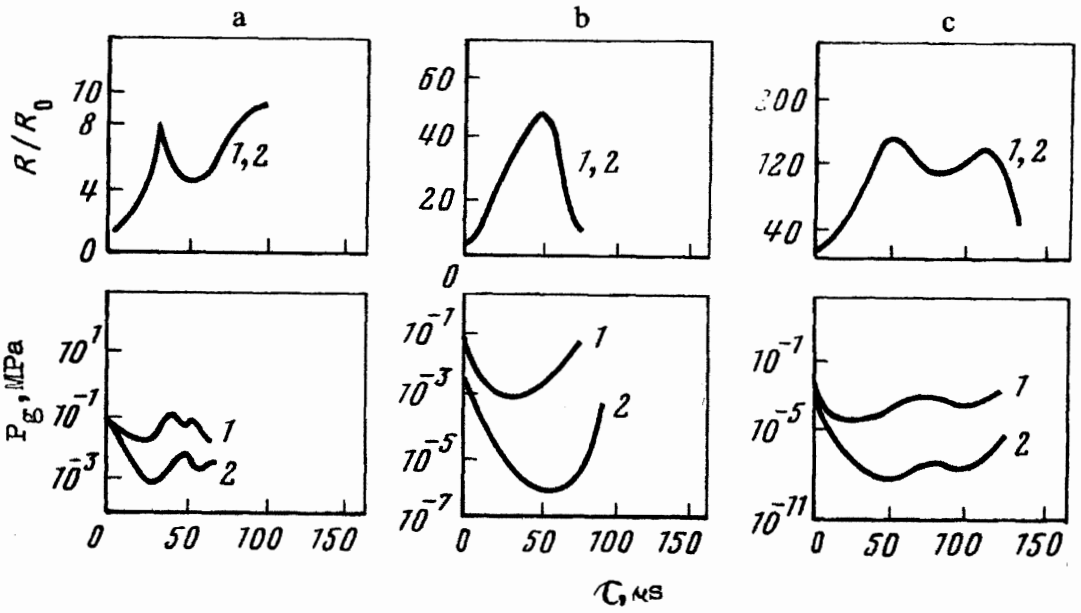


**Figure 1** Dynamics of cavitation bubbles in aluminium melt during ultrasonic treatment of various intensity. Initial bubble radius $R_0 = 10$ $\mu$m; sound pressure $P_s =$ (a) 0.2, (b) 1.0 and (c) 10 MPa. Calculations were performed (1) taking account of hydrogen diffusion into the bubble and (2) without it

increases the gas pressure by almost six orders of magnitude.

We can conclude that the ultrasonic treatment changes dramatically the behaviour of fine hydrogen bubbles in liquid aluminium. Without applied ultrasound, these bubbles dissolve owing to the diffusion flow of hydrogen out of the bubbles to the melt[5,6]. However, the alternating sound pressure applied to the melt along with the cavitation facilities the growth of gaseous bubbles. The diffusion-induced growth of bubbles depends on the intensity of ultrasound treatment, in other words, on the magnitude of sound pressure, gas content and other parameters of the liquid metal.

## Ultrasonic degassing of light alloy melts

Experimental sstudies of cavitation development in light alloy melts and the effect of cavitation on the kinetics of hydrogen removal during ultrasonic treatment confirm the essential connection between cavitation and degassing.

*Figure 2* demonstrates the effect of ultrasound on commercial aluminium melt over a wide range of sound intensity. Three typical regions occur in this dependence. The formation of these regions can be considered in terms of cavitation development. Region I reflects the precavitation treatment; only slight degassing can be observed. Within region II, the degassing increases sharply and then stabilizes; this is the region of developing cavitation. Region III is the region of optimum treatment modes with active cavitation; the degassing efficiency increases linearly with increasing ultrasound intensity. In other words, the transition to cavitation modes provides for the efficient removal of hydrogen from the melt.

*Figure 3* shows kinetic curves of ultrasonic degassing. One can compare the efficiency of ultrasonic treatment (1–2 kg charge of a liquid Al–Si–Mg alloy) with other known techniques of degassing. Note that the ultrasonic treatment (2) is more appropriate than vacuum treatment (3). It is noteworthy that mutual vacuum and ultrasonic treatment (4) considerably facilitates hydrogen removal from the melt.

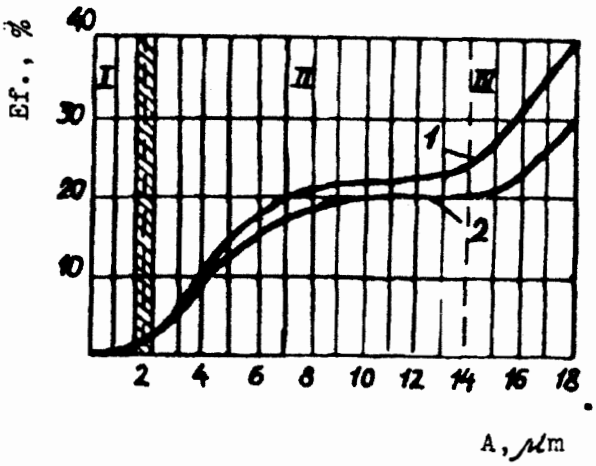


**Figure 2** Variation of the efficiency of ultrasonic degassing of (1) commercial A7 grade aluminium and (2) an industrial Al–6% Mg alloy with the intensity of ultrasonic treatment (oscillation amplitude of ultrasound source, *A*): I, no cavitation occurs; II, cavitation threshold; and III, developed cavitation

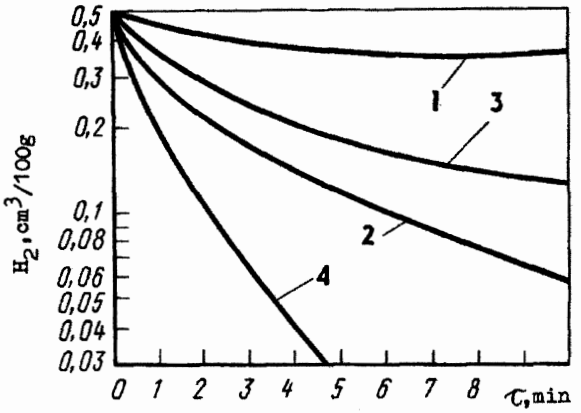


**Figure 3** Kinetics of hydrogen removal from an industrial Al–Si–Mg alloy during (1) processing with chlorine salts, (2) ultrasonic treatment, (3) vacuum treatment and (4) combined ultrasonic and vacuum treatment

We can distinguish the following regularities of degassing occurring under developed cavitation:

1 The nucleation of hydrogen bubbles occurs on the surface of non-wettable oxide particles in the sites of gas adsorption. This becomes possible only at sound pressures above the cavitation threshold.
2 Hydrogen bubbles grow owing to the directed diffusion of gas to the bubbles. The growth rate depends on the size of the initial nucleus, the starting content of hydrogen in the melt, the amplitude of sound pressure (i.e. ultrasound intensity and, hence, cavitation development) and the period of ultrasonic treatment.
3 Individual pulsating bubbles coagulate to form coarse macrobubbles owing to the action of the Bjerknes force and the development of acoustic microflows that are formed in the vicinity of pulsating bubbles.
4 The ultrasonic degassing results in the floating up of coarse hydrogen bubbles to the surface of the liquid bath. This process occurs due to the action of Stokes forces and with the aid of acoustic flows.

It should be noted that the bubble-aided hydrogen removal is accompanied by oxide flotation. In this case, the cavitation generates and develops on the non-wettable surface of these oxide particles. This effect can be easily observed when studying the fluidity of an Al–Si–Mg alloy melt[5], the fluidity (length of spiral) being 500 mm without treatment, 550 mm with argon blasting and 670 mm with ultrasonic degassing.

## Efficiency of ultrasonic degassing

The efficiency of ultrasonic-induced hydrogen removal from light alloy metals was thoroughly examined under industrial conditions. We also compared the ultrasonic degassing with other known techniques. *Table 1* shows the results obtained during different treatments of a liquid foundry Al–Si–Mg alloy. The highest efficiency achieved with ultrasonic degassing can be easily seen.

Industrial experiments performed during continuous casting of an Al–6% Mg alloy (ingot section 300 × 1700 mm; ultrasonic treatment of melt flow) showed that the cavitation treatment halves the content of hydrogen, from 0.6 to 0.3 $cm^3$ per 100 g (*Figure 4*). Similar results

**Table 1** Comparative efficiencies of industrial degassing techniques (150–300 kg charge; Al–Si–Mg alloy)

| Technique | $H_2$ ($cm^3$ per 100 g) | Density ($10^3$ kg $m^{-3}$) | Porosity number | UTS (MPa) | El (%) |
|---|---|---|---|---|---|
| Ultrasound | 0.17 | 2.706 | 1–2 | 245 | 5.1 |
| Vacuum | 0.20 | 2.681 | 1–2 | 228 | 4.2 |
| Argon blasting | 0.26 | 2.667 | 2–3 | 233 | 4.0 |
| Hexachloroethane | 0.30 | 2.663 | 2–3 | 212 | 4.5 |
| Flux | 0.26 | 2.660 | 3–4 | 235 | 4.0 |
| – | 0.35 | 2.660 | 4 | 200 | 3.8 |

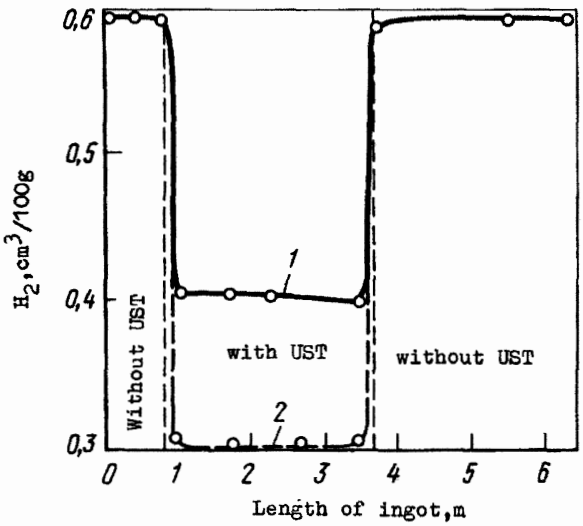


**Figure 4** Efficiency of ultrasonic degassing performed in a melt flow of an industrial Al–6% Mg alloy (flat ingots 300 × 1700 mm in section and 6 m long). Ultrasound power: (1) 9 and (2) 11 kW

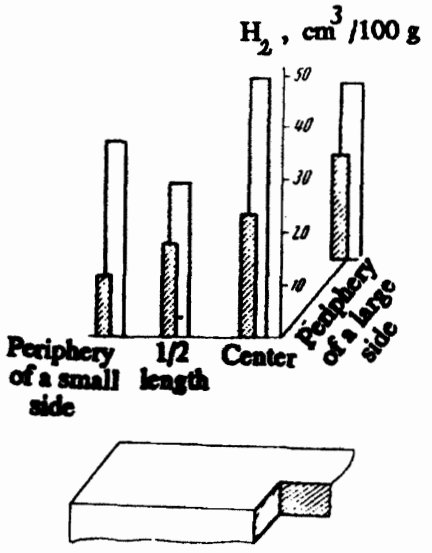


**Figure 5** Distribution of hydrogen across the section of a flat (550 × 165 mm) ingot of an industrial Mg–Al–Zn alloy: (1) without ultrasonic treatment and (2) after ultrasonic treatment (shaded bars)

**Table 2** Effect of ultrasonic degassing performed in a melt flow on the content of hydrogen and quality of 10 mm hot-rolled sheets of an Al–6% Mg alloy

| Property | Techniques of degassing | |
|---|---|---|
| | Conventional | Ultrasonic |
| $H_2$ ($cm^3$ per 100 g) | | |
| Melt | >0.60 | 0.30–0.33 |
| Ingot | 0.33–0.37 | 0.20–0.25 |
| Sheet | 0.30–0.34 | 0.18–0.22 |
| Density number | 2–3 | 1 |
| Ultimate tensile strength (MPa): | | |
| As-rolled | 193–235 | 239–247 |
| Annealed at high temperature | 69–80 | 170–206 |
| Fatigue endurance ($\times 10^5$ cycles to fracture) ($\sigma_{max}$ = 160 MPa) | 0.97–2.61 | 1.96–6.45 |

were obtained for magnesium alloys. *Figure 5* shows the distribution of hydrogen across the section of a flat Mg–Al–Zn alloy before and after ultrasonic treatment. The cleaning of the melt to remove gaseous and solid impurities during ultrasonic treatment improves considerably the quality of as-cast and deformed metal.

*Table 2* shows the effect of ultrasonic degassing on the content of hydrogen and the mechanical properties of an industrial Al–6% Mg alloy.

In recent years, we have developed a technique for combined cleaning of melt to remove both hydrogen and fine oxides (Usfirals process)[11]. This technique is based on a sonocapillary effect and capturing of solid inclusions in capillary channels of multilayer screen filters.

## Conclusions

The thorough investigation of ultrasonic melt degassing allowed us to establish an essential relationship between hydrogen removal and cavitation development. The developed cavitation increases the efficiency of ultrasonic degassing by 30–60%. Under optimum conditions, the ultrasonic degassing permits the hydrogen content in ingots and castings to be more than halved, improves the density and plasticity of as-cast metal with retained strength and increases the service reliability of deformed semifinished items.

## References

1 **Hiedemann, E.A.** Metallurgical effects of ultrasonic waves *J Acoust Soc Am* (1954) **26** 831
2 **Crowford, A.E.** *Ultrasonic Engineering* Butterworths, London, UK (1955)

3 **Eskin, G.I.** *Ultrasound in Metallurgy* Metallurgizdat, Moscow, USSR (1960) (in Russian)
4 **Campbell, J.** Effects of vibration during solidification *Int Met Rev* (1981) No. 1, 71
5 **Eskin, G.I.** *Ultrasonic Treatment of Molten Aluminium* 2nd edn Metallurgiya, Moscow, USSR (1988) (in Russian)
6 **Eskin, G.I. and Shvetsov, P.N.** An analysis of efficiency of ultrasonic degassing of a melt during continuous casting of aluminium alloy ingots, in: *Physical Metallurgy and Casting of Light Alloys* Metallurgiya, Moscow, USSR (1977) 17–31 (in Russian)
7 **Boguslavskii, Yu.Yu.** On gas diffusion into a cavity during cavitation *Akust Zh* (1967) **13** 23 (in Russian)
8 **Eskin, G.I.** *Processing and Quality Control of Nonferrous Alloys with Ultrasound* Metallurgiya, Moscow, Russia (1992) (in Russian)
9 **Eskin, G.I.** Laws of acoustic cavitation effect on the processes of aluminium and magnesium alloys refining and crytallization in the ultrasonic field, in: *Proceedings of International Symposium on Light Materials for Transportation Systems* Center for Advanced Aerospace Materials, Pohang, Korea (1993) 585–593
10 **Eskin, G.I.** Influence of cavitation treatment of melts in the processes of nucleation and growth of crystals during solidification of ingots and castings from light alloys *Ultrasonics Sonochem* (1994) **1** 59
11 **Eskin, G.I.** Fine filtration of the melts (Usfirals process), in: *Proceedings of International Conference on High Temperature Capillarity, Slovakia* (1994) 331